BRI Research Paper No. 62

#2060

NUMERICAL CALCULATION OF ROOM AIR MOVEMENT

ISOTHERMAL TURBULENT TWO DIMENSIONAL CASE

by

Takao TSUCHIYA

Building Research Institute
Ministry of Construction

JANUARY 1976

NUMERICAL CALCULATION OF ROOM AIR MOVEMENT
- ISOTHERMAL TURBULENT TWO-DIMENSIONAL CASE -

By Takao TSUCHIYA, Dr. Eng.**

SYNOPSIS

This paper presents a numerical calculation method for a two-dimensional, isothermal, turbulent room air movement. In this case, the time averaged stream function-vorticity equations were represented by finite differencing approximations with a box model and a leapfrog time scheme and the Reynolds stresses were assumed to be expressed in terms of an eddy kinematic viscosity which was estimated to be proportional to the product of the cube of a prescribed mixing length by a vorticity gradient.

This proportional constant was determined by comparing the computed velocity distributions with experiments for two basic flows. Furthermore, the parameterizations were proposed concerning the boundary conditions of vorticity on a wall which corrected the gaps between the true velocity and vorticity gradients and the represented by a finite differencing. These parameters were also determined as compared with experiments. Then, three obtained parameters were confirmed to be valid by applying to a rather complicated flow in which an air curtain was affected by a side blow.

CONTENTS

** Chief, Environmental Design Sect., Building Research Institute, Ministry of Construction

1. Introduction

Many successful results on the numerical calculations have been reported in every kind of field related to the fluid dynamics. Especially in meteorology, the conservative finite differencing schemes, such as Arakawa scheme[1], were devised free from the computational instability caused by the non-linear terms in order to make possible the long term prediction. As to the room air movement, there are several reports[2)-7)] which treat the laminar thermal convection in a room. However, there are very few[8)] which treat the turbulent room air movement with ventilation. It does not seem to be useless to make a brief review of the studies on the numerical calculation of the room air movement in our country at this moment.

First attempt[9)] was made in 1958 by Terai who treated the thermal convection in a room with a single heated wall. He succeeded in the integration of Navier-Stokes equations and Energy equation by Cowley-Levy method which expands the non-linear terms of N.S. equation in a power series by the same parameter as Grashof number and made an approximate integration successively. However, he described that Grashof number was limited under 3×10^3 to get stable solution.

In 1968, Tsuchiya[10)] tried to apply the finite difference numerical method with ventilation by a successive over- relaxation method. The serious problem encountered in the course of the study was that the calculation was stable only under low Reynolds number, $Re \leq 750$.

In 1972, Yamazaki[11)] succeeded in getting a stable solution up to Re=2000. His idea is to increase Re number a little bit and the same time to decrease relaxation parameter at every iteration procedure.

The flow is restricted only to laminar in all cases above described. However, the flow is essentially turbulent in a room even small box. Consequently, it is necessary to deal with turbulence in a computation. Some approximate methods were devised to compute a turbulent air convection. Tsuchiya[12)] adopted the same computing method as was used in a laminar case, assuming that eddy kinematic viscosity was constant in a whole area except the portion of quite vicinity of walls. Considering the fact that the maximum velocity and temperature appear at quite vicinity of walls, the computing domain was expanded so that the computed maximum velocity takes place on rigid boundary walls. In this case, the following relation was used as thermal boundary condition.

$$-\lambda a p \left(\frac{\partial T}{\partial n}\right)_w = \frac{1}{r}(T_w - T_o)$$

where, λ_{ap} ; apparent thermal conductivity

r ; thermal resistance between inner surface and outside

T_w ; inner surface temperature

T_o ; outside air temperature

Enai[13)] carried out the computation of the thermal convection with a sigle heated wall by dividing a domain into two regions at the point of maximum velocity where he made slip condition.

Recently, Kaizuka et. al.[14)] have gotten a good result for turbulent three-dimensional motion with ventilation by applying the Marker and Cell method and the two-equation model for turbulence.

The N-S eqn. governs not only laminar but also turbulent flow in its nature. However, a very fine mesh spacing will be required to resolve the minimum eddy by means of the finite differencing based on the N-S eqn. Therefore, it does not seem to be appropriate from the practical point of view. It appears to be the most applausible method to evaluate the contributions of the turbulence to the mean flow by means of an eddy kinematic viscosity. There are several methods[15), 16)] now available to estimate an eddy kinematic viscosity.

In this study, the computer programming of the numerical calculation for two- dimensional room air movements is developed by means of the box model finite differencing scheme for advection terms and the leapfrog scheme for time steps in the time averaged stream function-vorticity equations, together with the simplest method of the estimation of an eddy kinematic viscosity by a prescribed mixing length distribution.

The objective of this report is to find the most suitable values of three parameters γ, C_1 and C_2, where γ denotes an emperical constant in connection with an eddy kinematic viscosity and the product of the cube of a prescribed mixing length by the absolute value of a vorticity gradient and C_1, C_2 are the correcting coefficients which correct the discrepancy between the true and the represented by a finite differencing concerning the velocity and the vorticity gradient on a wall, respectively.

These parameters are determined by comparing the computed velocity distributions with experiments in a square and a rectangular cross sectional rooms with a low side wall outlet and a high side wall inlet. It is confirmed that these parameters are valid even for a complicated case in which an air curtain is affected by a side blow by comparing the computed flow patterns and velocity distributions with experiments. In an experimental setup, not only the measurements of air velocity but also the flow visualization are attempted.

2. Method of Numerical Calculation

2-1 Basic Equations

(i) Governing Equations

Well-known Navier-Stokes equations are as follows which govern two-dimensional room air motion.

$$\frac{\partial u}{\partial t} + u\frac{\partial u}{\partial x} + v\frac{\partial u}{\partial y} = -\frac{1}{\rho}\cdot\frac{\partial p}{\partial x} + \nu\left(\frac{\partial^2 u}{\partial x^2} + \frac{\partial^2 u}{\partial y^2}\right) \qquad \cdots\cdots\cdots\cdots (1)$$

$$\frac{\partial v}{\partial t} + u\frac{\partial v}{\partial x} + v\frac{\partial v}{\partial y} = -\frac{1}{\rho}\cdot\frac{\partial p}{\partial y} + \nu\left(\frac{\partial^2 v}{\partial x^2} + \frac{\partial^2 v}{\partial y^2}\right) \qquad \cdots\cdots\cdots\cdots (2)$$

Assuming that the room air would be incompressible, the equation of continuity can be expressed in the following form.

$$\frac{\partial u}{\partial x} + \frac{\partial v}{\partial y} = 0 \qquad \cdots\cdots\cdots\cdots (3)$$

Although $u, v, p,$ can be solved directly from Eqs. (1), (2) and (3), the transformed vorticity (Ω)-stream function (Ψ) equations will be adopted instead of Eqs. (1) - (3). These equations are:

$$\frac{\partial \Omega}{\partial t} + u\frac{\partial \Omega}{\partial x} + v\frac{\partial \Omega}{\partial y} = \nu\left(\frac{\partial^2 \Omega}{\partial x^2} + \frac{\partial^2 \Omega}{\partial y^2}\right) \qquad \cdots\cdots\cdots\cdots (4)$$

$$u = \frac{\partial \Psi}{\partial y}, \qquad v = -\frac{\partial \Psi}{\partial x} \qquad \cdots\cdots\cdots\cdots (5)$$

$$\Omega = -\left(\frac{\partial^2 \Psi}{\partial x^2} + \frac{\partial^2 \Psi}{\partial y^2}\right) \qquad \cdots\cdots\cdots\cdots (6)$$

In almost cases, the room air flow is considered to be turbulent. We can get the following vorticity equations for turbulent case by averaging the whole equations (4), (5) and (6) with substitution of

$$\Omega = \bar{\Omega} + \Omega'$$

$$u = \bar{u} + u'$$

$$v = \bar{v} + v'$$

$$\Psi = \bar{\Psi} + \Psi'$$

where over barred and dashed quantities indicate time averaged values and the deviation from them, respectively.

$$\frac{\partial \bar{\Omega}}{\partial t} + \bar{u}\frac{\partial \bar{\Omega}}{\partial x} + \bar{v}\frac{\partial \bar{\Omega}}{\partial y} = \frac{\partial}{\partial x}\left\{(Kx+\nu)\frac{\partial \bar{\Omega}}{\partial x}\right\} + \frac{\partial}{\partial y}\left\{(Ky+\nu)\frac{\partial \bar{\Omega}}{\partial y}\right\} \cdots\cdots(7)$$

where $\overline{u'\Omega'} = -Kx\frac{\partial \bar{\Omega}}{\partial x}$, $\overline{v'\Omega'} = -Ky\frac{\partial \bar{\Omega}}{\partial y}$

$$\bar{u} = \frac{\partial \bar{\Psi}}{\partial y}, \quad \bar{v} = -\frac{\partial \bar{\Phi}}{\partial x} \quad \cdots\cdots\cdots\cdots (8)$$

$$\bar{\Omega} = \frac{\partial \bar{v}}{\partial x} - \frac{\partial \bar{u}}{\partial y} \quad \cdots\cdots\cdots\cdots (9)$$

The bar sign over each variable will be omitted hereafter for simplicity. It is seen that Eqs. (8) and (9) are formally identical with Eqs. (5) and (6), respectively, if u, v, Ψ, Ω are replaced by their time-averages. In Eq. (7) $\overline{u'\Omega'}$ and $\overline{v'\Omega'}$ are assumed to be expressed in the terms of eddy kinematic viscosity and gradient of vorticity. In addition, assuming that the eddy kinematic viscosity Kx, Ky can be coupled with the mixing length and the vorticity gradient, then the following expressions are possible.

$$Kx = \gamma \ell^3 \left|\frac{\partial \Omega}{\partial x}\right|, \quad Ky = \gamma \ell^3 \left|\frac{\partial \Omega}{\partial y}\right| \quad \cdots\cdots\cdots\cdots (10)$$

where, γ : emperical constant

ℓ : mixing length

Eqs. (7) - (10) give a complete set for computation explicitly with the aid of following boundary conditions.

(ii) Boundary Conditions

Non-slip condition $u = v = 0$ is imposed on all wall surfaces except the portion of outlet and inlet where uniform velocity, i. e. linear distribution of Ψ will be given. This is transformed into the following relations in terms of vorticity.

(1) $\Omega w = -\left(\frac{\partial u}{\partial n}\right)_w$ $\cdots\cdots\cdots\cdots$ (11)

(2) $(\Omega\, flux)_w = \nu\left(\frac{\partial \Omega}{\partial n}\right)_w$ $\cdots\cdots\cdots\cdots$ (12)

2-2 Finite Difference Approximation by Box Model[17)]

(i) Stream Function-Vorticity Equations

We adopt the Box Model as a finite differencing scheme for advection terms because of following reasons.

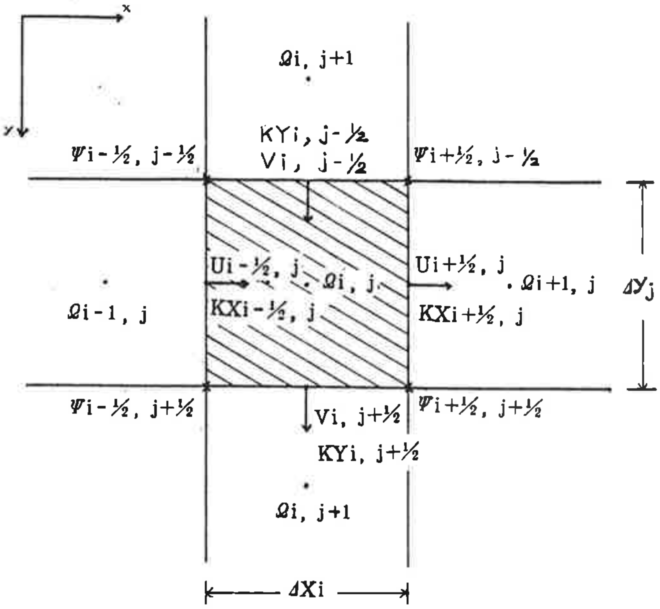

Fig. 1 Grid Arrangement of Box Model

(1) In almost room air motions, the distribution of velocity or temperature indicates a strong and sharp change at the quite vicinity of walls, whilist a rather moderate change at the central area of a room. Therefore, when a regular mesh spacing would be used, a fine mesh spacing should be required to resolve the whole field. However, this is not economical from the point of core memory and CPU time. Consequently, an irregular mesh spacing is desirable which covers the whole space with fine mesh spacing for near a wall and coarse for central area.

(2) Computational instability does not occur even if the irregular mesh spacing may be used, because the aliasing is controlled that the quadratic quantity Ω^2 for nonlinear terms is devised to be conserved when summed over all grid points in a domain. Aliasing is considered to happen when waves that are too short to resolved by given set of grid points are misrepresented by long waves. Uncontrolled aliasing causes computational instability until divergence takes place.

We consider the area surrounded by lattice grids as a box, and define the vorticity Ω at the center of a box and the stream function Ψ on the grid point as shown in Fig. 1. Then, velocities are reduced to be defined on the boundary surfaces adjacent to the surrounding boxes. Consequently, we can estimate the advective transportation of scalar quantity such as a mean vorticity $\frac{\Omega_{i,j}+\Omega_{i-1,j}}{2}$ on these surfaces. In addition, assuming that the distribution of vorticity between adjacent boxes is linear, we can get the following equations expressed in the finite difference approximations for Eqs. (7) - (10).

$$\frac{\Omega_{i,j}^{n+1}-\Omega_{i,j}^{n-1}}{2\Delta\tau}\Delta x_i\Delta y_j+\left(u_{i+\frac{1}{2},j}\frac{\Omega_{i+1,j}+\Omega_{i,j}}{2}-u_{i-\frac{1}{2},j}\frac{\Omega_{i,j}+\Omega_{i-1,j}}{2}\right)^n\Delta y_j$$

$$+\left(v_{i,j+\frac{1}{2}}\frac{\Omega_{i,j+1}+\Omega_{i,j}}{2}-v_{i,j-\frac{1}{2}}\frac{\Omega_{i,j}+\Omega_{i,j-1}}{2}\right)^n\Delta x_i$$

$$=\left\{KX_{i+\frac{1}{2},j}\frac{\Omega_{i+1,j}-\Omega_{i,j}}{\frac{1}{2}(\Delta x_{i+1}+\Delta x_i)}-KX_{i-\frac{1}{2},j}\frac{\Omega_{i,j}-\Omega_{i-1,j}}{\frac{1}{2}(\Delta x_i+\Delta x_{i-1})}\right\}^{n-1}\Delta y_j$$

$$+\left\{KY_{i,j+\frac{1}{2}}\frac{\Omega_{i,j+1}-\Omega_{i,j}}{\frac{1}{2}(\Delta y_{j+1}+\Delta y_j)}-KY_{i,j-\frac{1}{2}}\frac{\Omega_{i,j}-\Omega_{i,j-1}}{\frac{1}{2}(\Delta y_j+\Delta y_{j-1})}\right\}^{n-1}\Delta x_i \quad \cdots\cdots\cdots \quad (13)$$

where,

$$\left.\begin{aligned} u_{i+\frac{1}{2},j}&=\frac{\Psi_{i+\frac{1}{2},j+\frac{1}{2}}-\Psi_{i+\frac{1}{2},j-\frac{1}{2}}}{\Delta y_j}, \quad u_{i-\frac{1}{2},j}=\frac{\Psi_{i-\frac{1}{2},j+\frac{1}{2}}-\Psi_{i-\frac{1}{2},j-\frac{1}{2}}}{\Delta y_j}\\ v_{i,j+\frac{1}{2}}&=\frac{\Psi_{i-\frac{1}{2},j+\frac{1}{2}}-\Psi_{i+\frac{1}{2},j+\frac{1}{2}}}{\Delta x_i}, \quad v_{i,j-\frac{1}{2}}=\frac{\Psi_{i-\frac{1}{2},j-\frac{1}{2}}-\Psi_{i+\frac{1}{2},j-\frac{1}{2}}}{\Delta x_i}\end{aligned}\right\} \quad (14)$$

$$\Omega_{i+\frac{1}{2},j+\frac{1}{2}}=\left\{\frac{2}{(\Delta x_{i+1}+\Delta x_i)\Delta x_{i+1}}+\frac{2}{(\Delta x_{i+1}+\Delta x_i)\Delta x_i}+\frac{2}{(\Delta y_{j+1}+\Delta y_j)\Delta y_{j+1}}+\frac{2}{(\Delta y_{j+1}+\Delta y_j)\Delta y_j}\right\}$$

$$\Psi_{i+\frac{1}{2},j+\frac{1}{2}}-\left\{\frac{2\Psi_{i+\frac{3}{2},j+\frac{1}{2}}}{(\Delta x_{i+1}+\Delta x_i)\Delta x_{i+1}}+\frac{2\Psi_{i-\frac{1}{2},j+\frac{1}{2}}}{(\Delta x_{i+1}+\Delta x_i)\Delta x_i}+\frac{2\Psi_{i+\frac{1}{2},j+\frac{3}{2}}}{(\Delta y_{j+1}+\Delta y_j)\Delta y_{j+1}}-\frac{2\Psi_{i+\frac{1}{2},j-\frac{1}{2}}}{(\Delta y_{j+1}+\Delta y_j)\Delta y_j}\right\} \quad (15)$$

The grid point vorticity $\Omega_{i+\frac{1}{2},j+\frac{1}{2}}$ may be estimated by averaging four vorticity values surrounding that point.

$$\Omega_{i+\frac{1}{2},j+\frac{1}{2}}=(\Omega_{i+1,j+1}+\Omega_{i,j+1}+\Omega_{i,j}+\Omega_{i+1,j})/4 \quad \cdots\cdots\cdots \quad (16)$$

$$\left.\begin{aligned} KX_{i+\frac{1}{2},j}&=\gamma\ell^3\left|\frac{\Omega_{i+1,j}-\Omega_{i,j}}{\frac{1}{2}(\Delta x_{i+1}+\Delta x_i)}\right|+\nu\\ KY_{i,j+\frac{1}{2}}&=\gamma\ell^3\left|\frac{\Omega_{i,j+1}-\Omega_{i,j}}{\frac{1}{2}(\Delta y_{j+1}+\Delta y_j)}\right|+\nu\end{aligned}\right\} \quad \cdots\cdots\cdots\cdots \quad (17)$$

In Eq. (13), we made use of the centered (leap-frog) time scheme for the marching term. A leap-frog time difference involves at three time levels and this introduces a non-physical computational mode into the solution. The mode takes the form of an oscillation about the true solution with respect to the even and odd time steps. This causes the instability referred as 'time splitting'. However, provided the instbility remains small, Lilly[19] has shown that the leap-frog time scheme would be very accurate as compared with analytical solutions among other time differencing schemes which displayed an undesirably strong damping of the kinetic energy. Thus the leap-frog scheme is preferable if the weak instability can be controlled. This can be done by starting the time step with the initial value and the value gotten by the combination of Forward and Centered schemes.

It is also well-known property of a leap-frog time scheme that causes a computational instability when coupled with the viscous terms.[20] In order to remove this instability, the simple lagging of one time step was employed for the diffusion terms indicated by superscript n-1.

Stability criterion for marching step is roughly evaluated by

$$\Delta\tau < \frac{\Delta x_{min} \text{ or } \Delta y_{min}}{|u_{max}| + |v_{max}|} \qquad \cdots\cdots\cdots\cdots (18)$$

ii) Boundary Conditions

Boundary conditions on wall surfaces can be written in the finite difference form by (Fig. 2)

(1)
$$\Omega_w = -\frac{c_1}{2}\left(\frac{u_1}{\frac{1}{2}\Delta y_1} + \frac{u_{-1}}{\frac{1}{2}\Delta y_1}\right) \qquad \cdots\cdots\cdots\cdots (19)$$

(2)
$$(\Omega_{flux})_w = c_2 \nu \frac{\Omega_1 - \Omega_w}{\frac{1}{2}\Delta y_1} \qquad \cdots\cdots\cdots\cdots (20)$$

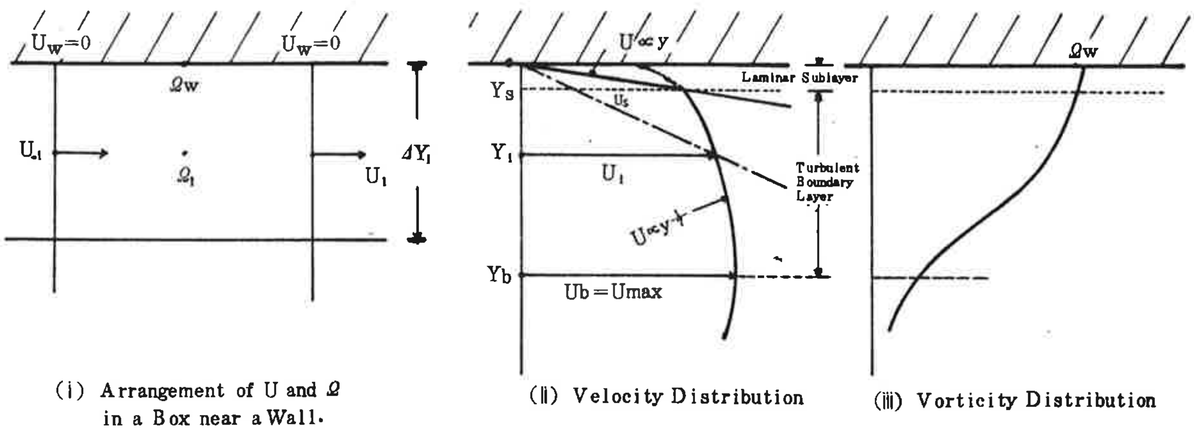

Fig. 2 Schematic Display of Variation of Velocity and Vorticity near a Wall

In above two equations, we propose two coefficients c_1, c_2 which correct the discrepancy between the actually existing gradients of velocity and vorticity in a laminar sublayer and the represented by a first order finite differencing in the box close to a wall.

These correction are inevitable because it might be impossible from the point of computer economy to use so small mesh spacing as to resolve a laminar sublayer. These coefficients will be given in later section.

2-3 Computational Procedure

We now list the basic steps in the computational procedure.

Step (1) Set the initial value of $\Omega^{\circ}_{i,j}$ for all interior points and also set Ψ value on all boundaries

Step (2) Solve Poisson type Eq. (15) to get $\Psi_{i,j}$ for interior grid points

Step (3) Calculate u, v, KX and KY from Eqs. (14) and (17)

Step (4) Calculate Ω_w and $(\Omega_{flux})_w$ from Eqs. (19) and (20)

Step (5) Obtain $\Omega_{i,j}$ advanced one time step from Eq. (13)

Step (6) At the next time step, repeat steps (2) - (5)

In step (1), the initial guess of $\Omega_{i,j}$ is made. The computational time required to reach steady state is quite dependent on whether the initial guess is good or not. We estimate this value as $\frac{U_0}{2} \times \frac{H}{2}$, where U_0 and H are the outlet air velocity and the height of a room, respectively. In step (2), we make use of the successive over-relaxation method to solve Poisson type equation. Iterative scheme can be written in the following form by transforming Eq. (15).

$$\Psi^{k+1}_{i+\frac{1}{2},\,j+\frac{1}{2}} = \Psi^{k}_{i+\frac{1}{2},\,j+\frac{1}{2}} + (1+\alpha)\Big[\frac{1}{A}\Big\{\frac{2\Psi_{i+\frac{3}{2},\,j+\frac{1}{2}}}{(\triangle x_{i+1}+\triangle x_i)\triangle x_{i+1}} + \frac{2\Psi_{i-\frac{1}{2},\,j+\frac{1}{2}}}{(\triangle x_{i+1}+\triangle x_i)\triangle x_i}$$

$$+\frac{2\Psi_{i+\frac{1}{2},\,j+\frac{3}{2}}}{(\triangle y_{j+1}+\triangle y_j)\triangle y_{j+1}} + \frac{2\Psi_{i+\frac{1}{2},\,j-\frac{1}{2}}}{(\triangle y_{j+1}+\triangle y_j)\triangle y_j} + \Omega_{i+\frac{1}{2},\,j+\frac{1}{2}}\Big\} - \Psi^{k}_{i+\frac{1}{2},\,j+\frac{1}{2}}\Big] \cdots\cdots \quad (21)$$

where, $A = \frac{2}{\triangle x_{i+1}\,\triangle x_i} + \frac{2}{\triangle y_{j+1}\,\triangle y_j}$

α : acceleration parameter (= 0.7 - 0.9)

k : number of iteration

It might be preferable to change the direction of iterative process, because this causes dispersion of truncation errors in all points evenly so that the accumulation of errors can be avoided.

In step (5), we use the leapfrog time scheme, as described earlier, which causes the computational instability by increase of computational mode. We intend to suppress the progress of computational mode by the following process which is believed to be best method today as shown in Fig. 3.

1. Guess Ω^{05} by the forward time scheme using the initial value Ω^0
2. Obtain Ω^1 by the centered time scheme using Ω^0 and Ω^{05}
3. Obtain Ω^2 by the centered time scheme using Ω^0 and Ω^1
4. In general, obtain Ω^{n+1} by the centered time scheme using Ω^{n-1} and Ω^n for $n = 2, 3, \ldots$

Furthermore, we restart the above described process at every 30 time steps.

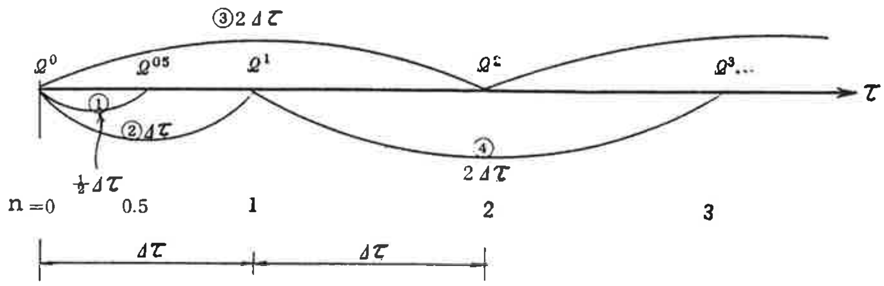

Fig. 3 Step of Time Extrapolation for Leapfrog Scheme

3. Cases and Conditions of Calculation

3-1 Cases of Calculation

We carried out the numerical calculation for four cases.

Case 1 is for the air motion in the room with square cross section represented by 1.5m height. The outlet and inlet are located at the right side wall. The former is on the floor level and the latter on the ceiling, respectively. These have the same slot type opening of 0.05 m x 1.5 m. The outlet air velocity is 3.0 m/s.

Case 2 is all the same as Case 1 except the room aspect ratio of 2.2 and the outlet air velocity of 1.7 m/s.

In Case 1 and 2, six kind of calculations were carried out making use of different combinations of C_2 and γ. The most suitable values of C_2 and γ will be determined as compared with experimental results.

Case 3 is for the air motion in the room with aspect ratio of 2.2 possessing the outlet on the center of the ceiling and the inlet on the center of the floor. Let we call it an "air curtain". The outlet air velocity is 3.4 m/s.

Case 4 is for the air motion of the air curtain with 3.4 m/s outlet velocity affected by the side blow which penetrates along the floor from the right side wall opening by 1.7 m/s outlet velocity.
In these cases, the outlet and inlet are all the same slot type as Case 1.

Those are summarized briefly in Table 1.

3-2 Conditions of Calculation

(1) Grid System

Fig. 4 shows the grid systems which were used in the calculation of each case.

It can be observed that an irregular mesh spacing, fine for near a wall and jet regions and sparse for central area of a room, is used. The finest mesh space normalized by room height for each case but 2 is 0.008, which corresponds

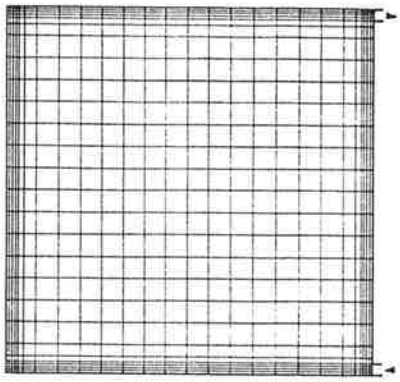

Case 1

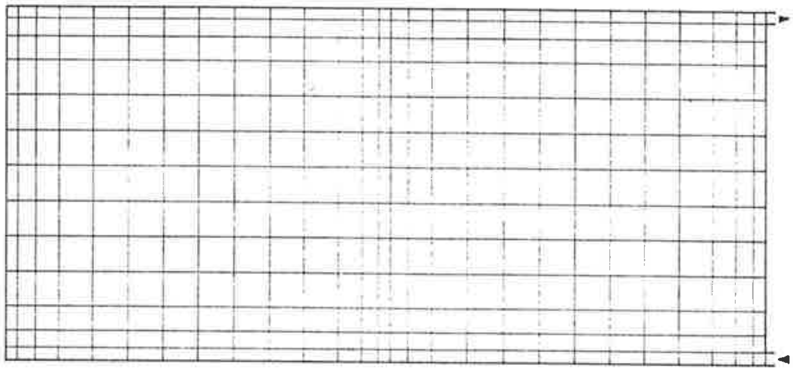

Case 2

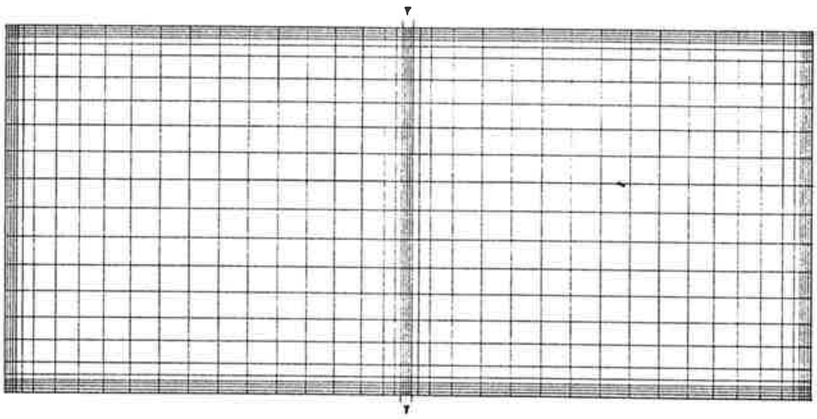

Case 3

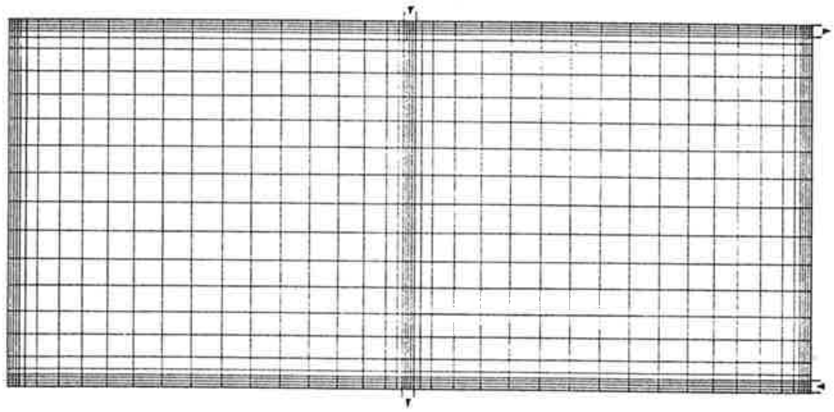

Case 4

Fig. 4　Grid Systems for Each Case

Table 1. Cases and Conditions of Calculation

Case NO.	Arrangement of Outlet and Inlet	Combination of r, C_2 and ℓ					Outlet Air Velocity	Smallest Mesh Spacing
			r	C_2	mixing length Type	isotropic or non-isotropic		
1	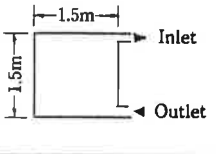	(i)	4	0.1	I	isotropic	3.0 m/s	12mm
		(ii)	4	1.0	I	〃		
		(iii)	4	1.0	II	non-isotropic		
		(iv)	1	0.1	II	〃		
2	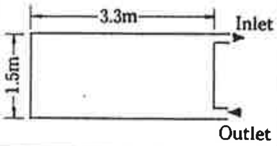	(i)	1	1.0	II	non-isotropic	1.7	50
		(ii)	4	1.0	I	isotropic		
3	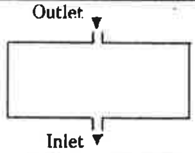		1	0.1	II	non-isotropic	3.4	12
4	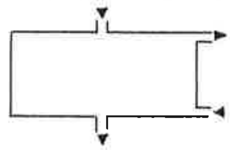		1	0.1	II	〃	3.4 (air curtain) 1.7 (side blow)	12

to the quarter of the outlet width. In case 2, the finest mesh space is four times larger than the other cases. It is set in order to verify the resolutional limitation according to the mesh spacing.

(2) Time Increment $\Delta\tau$

Dimensionless time increment $\Delta\tau$ was selected to satisfy the stability criterion Eq. (18) as follows.

$$\Delta\tau = \frac{\Delta x\,,\Delta y_{min}}{|u|_{max} + |v|_{max}} = \frac{0.008}{2}$$

However, this caused the strong instability to divergence after the first several time steps in the preliminary calculations. Consequently, one tenth value was used for the first several time steps.

(3) Estimation of Correcting Coefficient C_1

Providing that the turbulent flow near a wall of the room air motion might be represented by the smooth flat plate flow, the thickness of the laminar sublayer is given by the emperical relation [21] as

$$y_s = \frac{5\nu}{\sqrt{\tau_w/\rho}} \qquad \cdots\cdots\cdots\cdots (22)$$

$$\tau_w/\rho = 0.0225\, u_b^2 \left(\frac{\nu}{u_b\, y_b}\right)^{1/4} \qquad \cdots\cdots\cdots (23)$$

where, y_s : thickness of laminar sublayer

ν : kinematic viscosity

ρ : density

τ_w : wall shearing stress

Furthermore, 1/7-th power law is assumed for the velocity profile of the boundary layer near a wall except a laminar sublayer where the mean velocity increases linearly with distance from the wall. Boundary layer thickness y_b is defined as the distance from the wall to the point where the calculated velocity becomes maximum. Then the following relations are gotten in reference with Fig. 2.

$$\frac{u_s}{u_b} = \left(\frac{y_s}{y_b}\right)^{1/7}$$

$$\frac{u_1}{u_b} = \left(\frac{y_1}{y_b}\right)^{1/7} \qquad \therefore \qquad \left(\frac{\partial u}{\partial y}\right)_w = \frac{u_s}{y_s} = \left(\frac{y_1}{y_s}\right)\frac{u_1}{y_1} \qquad \cdots\cdots\cdots (24)$$

Therefore, one can obtain C_1 as

$$C_1 = \left(\frac{y_1}{y_s}\right)^{6/7} \qquad \cdots\cdots\cdots (25)$$

(4) Correcting Coefficient C_2

When the linear velocity profile is assumed in a laminar sublayer, vorticity near a wall will take a constant value because the vorticity in that region approximately equals to the velocity gradient normal to the wall. Therefore, the vorticity gradient at the wall $\left(\frac{\partial \Omega}{\partial n}\right)_w$ will reduce to be near zero. The coefficient C_2 was proposed in order to correct the discrepancy between the actual vorticity gradient at the wall and the finite differencing approximation. In Case 1 and 2, three kinds of values $C_2 = 0.1, 0.5, 1.0$ are used. The most suitable value will be selected as compared with the later experimental results.

(5) Emperical Constant γ for Eddy Kinematic Viscosity

We assumed that the eddy kinematic viscosity was proportional to the product of the absolute value of local vorticity gradient and the cube of mixing length. To estimate the eddy kinematic viscosity according to Eq. (17), the value of γ must be given. Four values 0.1, 0.4, 1.0, 4.0 are provided to select the best fit for the numerical calculation.

(6) Mixing Length ℓ

According to the knowledge of smooth pipe flows,[21] the variation of mixing length over the diameter of the pipe can be represented by the emperical relation

$$\frac{\ell}{R} = 0.14 - 0.08\left(1-\frac{y}{R}\right)^2 - 0.06\left(1-\frac{y}{R}\right)^4 \quad \cdots\cdots\cdots (26)$$

where, R : half the diameter of pipe

In the neighbourhood of the wall this equation can be simplified to

$$\ell = 0.4y - 0.44\frac{y^2}{R} + \cdots\cdots \quad \cdots\cdots (27)$$

Here, we propose two types of variation for mixing length over a room guessed from the findings of smooth pipes. They are given in Fig. 5. Whereas Type I is the simplified of the smooth pipe flows, Type II is based on the combination of two boundary layers, the wall boundary and the remaining boundary.

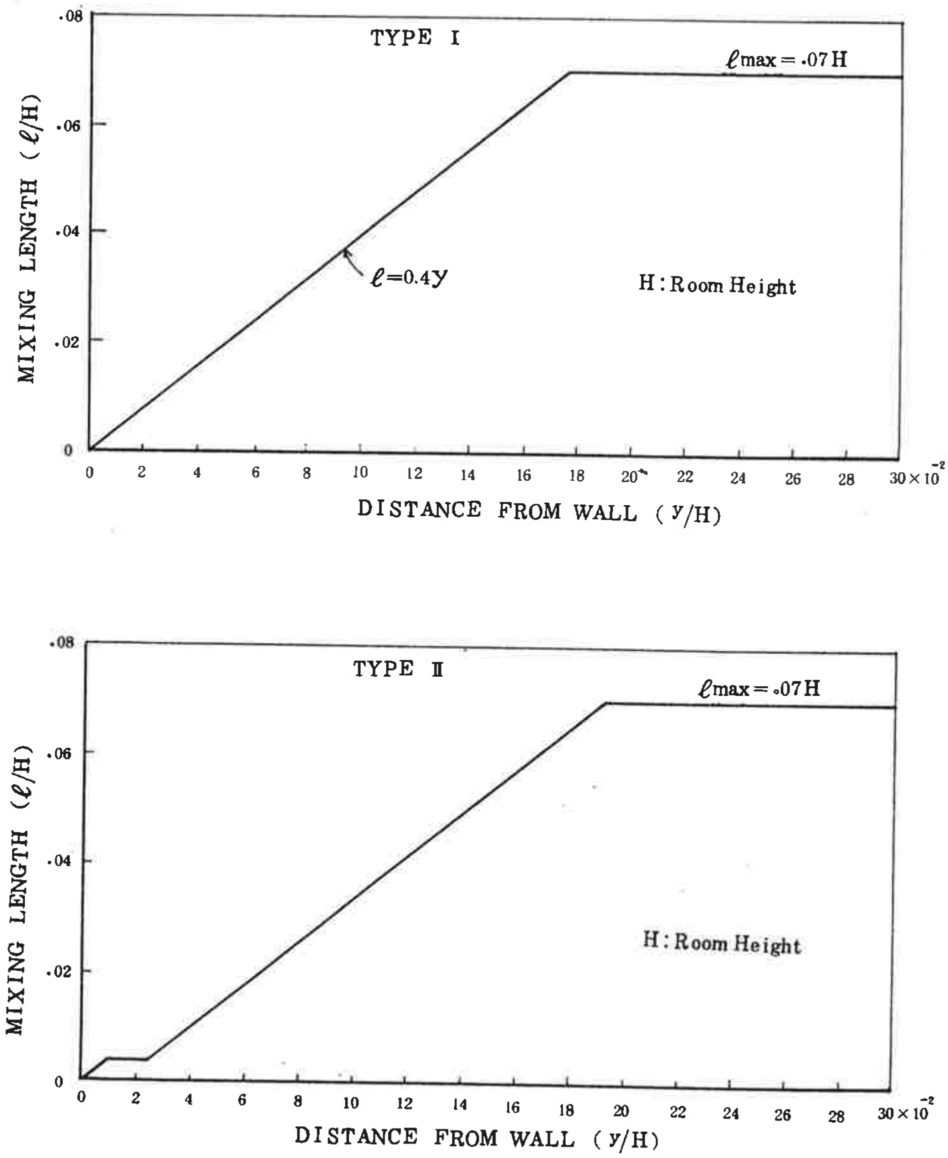

Fig. 5 Variation of Mixing Length

The maximum value of mixing length ℓ max can be estimated as

$$\ell_{max} = 0.14 \times \frac{H}{2} \qquad \cdots\cdots\cdots \quad (28)$$

where, H : height of a room

The shape of turbulence near a wall is considered to be oblong, which is referred as non-isotropic. Therefore, it is reasonable to assume that the variation of mixing length in the direction normal to the wall is represented by either Type I or II, on the other hand, that in the direction parallel to the wall is uniform and its value equals to ℓ max. On the contrary, isotropic means that the variation of ℓ is the same in both directions.

They are schematically displayed in Fig. 6.

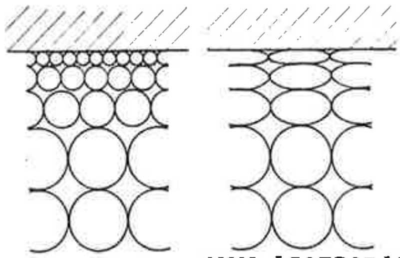

Fig. 6 Schematic View of Turbulence near a Wall

(7) Conditions for Outlet

a. Velocity Distribution

Uniform velocity distribution is assumed over the outlet opening. Then, linear distribution of Ψ is obtained.

b. Determination of C_1 and C_2

The coefficients C_1 and C_2 are strongly dependent on the shape, roughness, turbulence generator and so forth of the outlet. Therefore, these should be determined by experiment. In each calculation, these were decided by trial and error to make the computed decay curve of the center-line velocity near the outlet to be identical to the experimentally obtained for the wall jet with slot-type outlet.

c. Vorticity just outside of the Outlet Boxes

In order to calculate the vorticity of the outlet and inlet boxes, it is necessary to give the value just outside these boxes. All zero values are given so that the quadratic value of vorticity remains conserved when summed over whole domain for the non-linear terms.

(8) Conditions for Inlet

a. Velocity Distribution

Uniform velocity distribution is also assumed, which satisfy the continuity condition for the whole domain.

b. Determination of C_1 and C_2

C_1 and C_2 are set zero, that is, we neglect the contribution of the vorticity diffusion from the wall of the inlet.

c. Vorticity just outside of the Inlet Boxes

These are all set zero as described earlier.

4. Experiment

Measurements of air velocity and flow visualizations were carried out to verify the calculations for each case.

4-1 Test Rooms

Two basic test rooms were used. One was a square cross section, the other was a rectangular cross section, respectively. The former dimensions were 1.5 x 1.5 x 1.5 m, the latter were 3.3 x 1.5 x 1.5 m. The front wall and a part of the side wall were made of acrylic plate so that the observation of air flow was possible. Other walls were composed of veneer plate. The slot type with 1.5 x 0.05 m outlet and inlet were located at low and high sidewall. Especially, in a rectangular test room, there had another pair of outlet and inlet in the central area of ceiling and floor. These were used for an air curtain.

4-2 Assembly of Air Supply and Return System

The schematic view of supply and return system was shown in Fig. 7. The supplied air from the slot traveled through a test room, return air chamber, a packaged conditioner and a supply air chamber.

4-3 Method of Air Velocity Measurements

The air velocity at each measuring station was measured by moving the hot wire anemometers along a vertical and a horizontal guide pipes. For the measurement of air velocity higher than 0.2 m/s, Anemomaster Model 24-3111 of KANOMAX (Japan) was used and for lower than 0.2 m/s, Type 55 80/81 Low Velocity Anemometer of DISA (Denmark) was used.

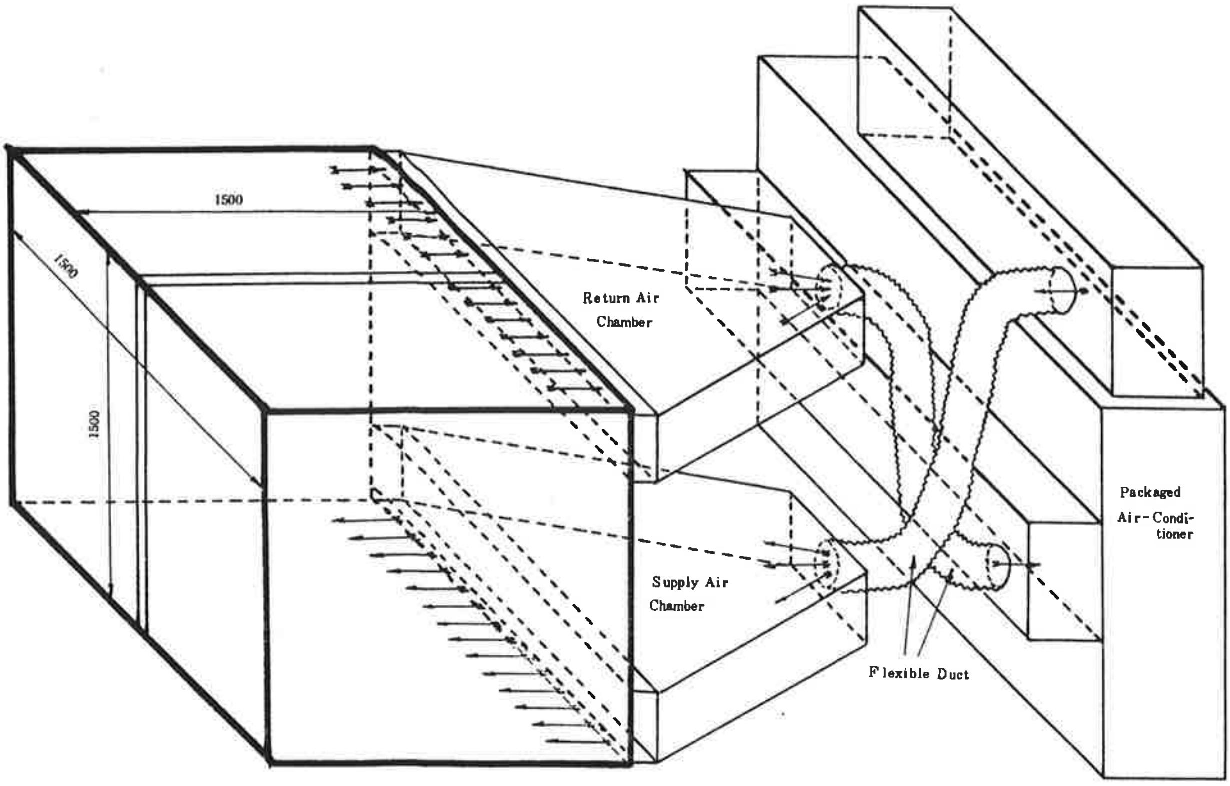

Case 1

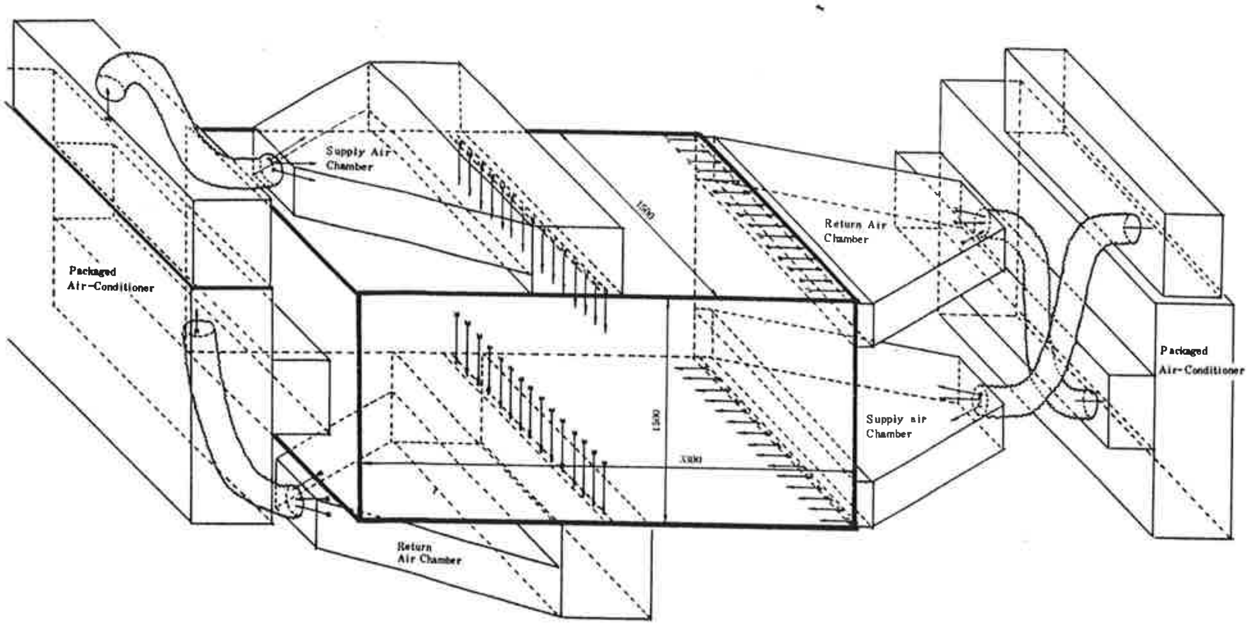

Case 4

Fig. 7 Schematic View of Supply and Return Air Systems

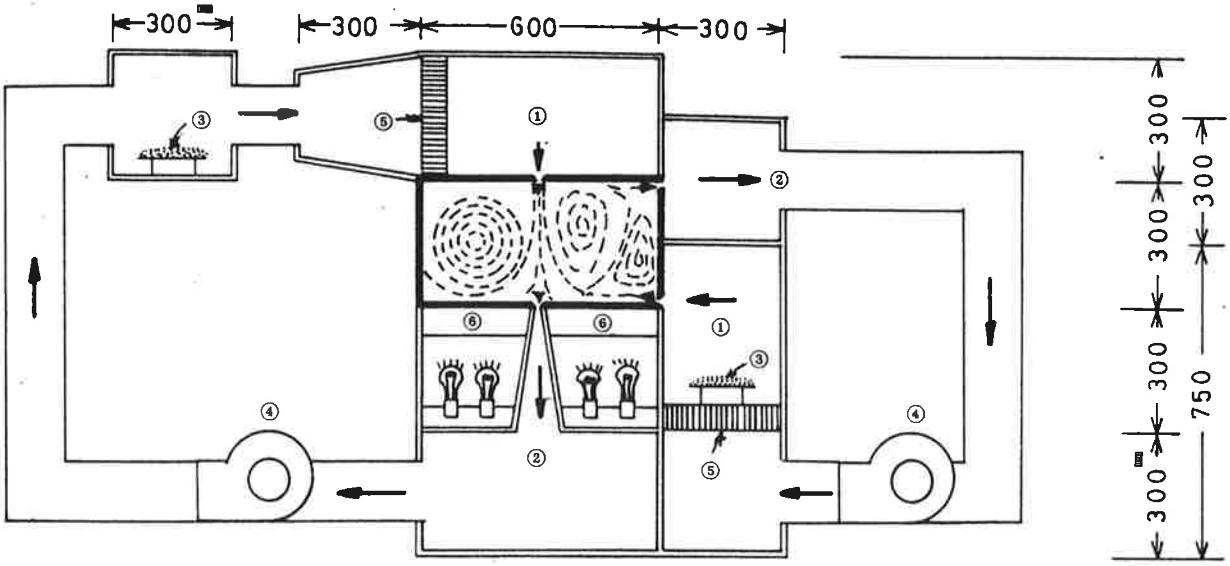

① Supply Air Chamber
② Return Air Chamber
③ Tracer Generator
(Metaldehyde)
④ Fan
⑤ Honeycomb Core
⑥ Illumination Box

Fig. 8 Arrangement of Apparatus for Visualization of Two-Dimensional Room Air Movements

4-4 Flow Visualization

The arrangement of an experimental apparatus for the flow visualization is shown in Fig. 8. It was composed of the 1/5 scale model of the test room, 0.6 m x 0.3 m in plan and 0.3 m high, two couples of outlet and inlet air chambers, the illumination box and the tracer generator boxes. They were connected by flexible ducts with two blowers.

The scale model was made of 12 mm veneer plate except the front wall and the part of the floor where 3 mm glass was used.

Particles of metaldehyde[22)] were used as visible tracers. The substance sublimes at about 100~120°C and then reverts to the solid phase to form light weight particles. These particles were continuously generated by heating the powder state metaldehyde feeded from outside.

The particles were illuminated by four pieces of a high beam lamp (500 w) set in an array mounted in the illumination box. The light was projected through the glass part with 1 cm width of the floor to take the pictures of two-dimensional air movement in the central plane. The time-exposure photographs were taken with different kinds of exposure time.

5. Results

5-1 Value of γ

The computations with different value of γ were carried out and then the following result was deduced. The value of γ strongly affected the computational stability, that is, when γ was 0.1 or 0.4, the computation was quite instable and the steady state solution was not obtained. On the contrary, when γ was 1.0 or 4.0, the steady state was attained in rather earlier stage of time steps.

The large discrepancy between two calculated velocity distributions in Fig. 10 might be mainly dependent on the difference of γ value. In case of $\gamma = 4$, the diffusion term took a considerable role and the excessive damping was encountered. Therefore, $\gamma = 1$ appears to be the most proper value.

5-2 Mixing Length

We assumed two types of distribution for mixing length ℓ. Type I was based on the assumption that the boundary layer was extended to the center of a room from the wall, and Type II was on the assumption that the influence of a wall was limited to the area within the point whose velocity took the maximum value and the flow was free turbulent within the area from this point to the center of a room.

In Fig. 10, the broken line represents the velocity distribution when Type I is used, whereas the solid line does when Type II is used. The former indicates a rather moderate curve at the region quite near a wall, on the contrary the latter indicates a steep variation. It is observed that the latter is more close to the experimental velocity distributions. In latter case, we assumed also non-isotropic model of turbulence. As it should be acceptable that the diffusion in the flow direction is quite small as compared with the advection in a turbulent boundary layer, the velocity distribution might be little affected by the assumption of isotropic or non-isotropic. Therefore, it seems to be dependent on the difference of ℓ distribution that the solid line reveals a steeper curve than the broken line.

5-3 Value of C_2

It can be seen from Fig. 9 that the velocity distribution near a wall is strongly affected by the value of C_2. In case of $C_2 = 1.0$, the variation of velocity over a wall indicates a moderate curve and the maximum velocity appears at the point quite far from a wall. On the other hand, in case of $C_2 = 0.1$, the maximum velocity appears at the point close to a wall and the overall velocity distribution agrees very well with the experimental result within a small deviation.

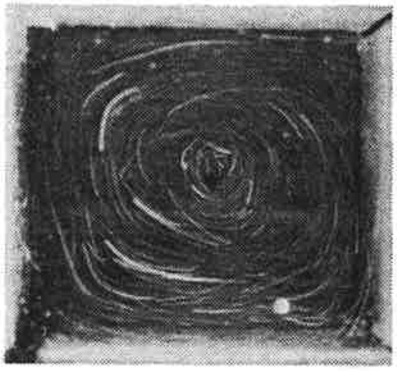

(a) Flow Pattern, $t = 1/4$ sec, $f = 2.0$

(a) Flow Pattern, $t = 1/2$, $f = 2.8$: 2.8

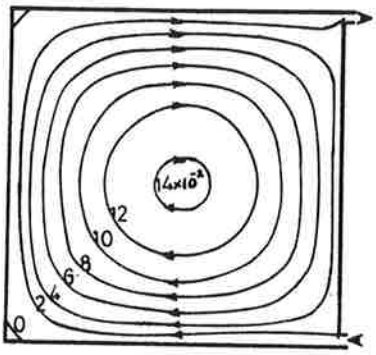

(b) Stream Function

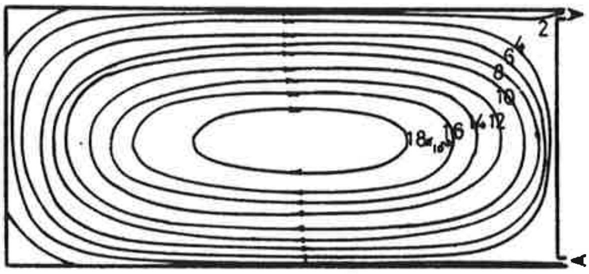

(b) Stream Function

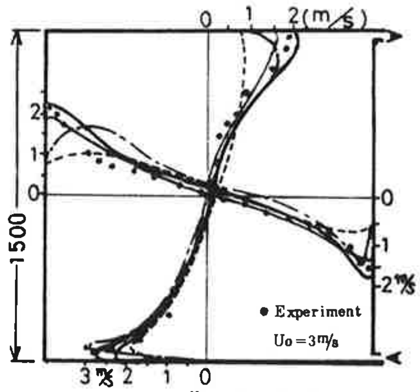

	r	C_2	ℓ-Type
(i) ———	4	0.1	I
(ii) - - - - - - -	4	1.0	I
(iii) — - —	4	1.0	II
(iv) ━━━	1	0.1	II

(c) Velocity Distributions

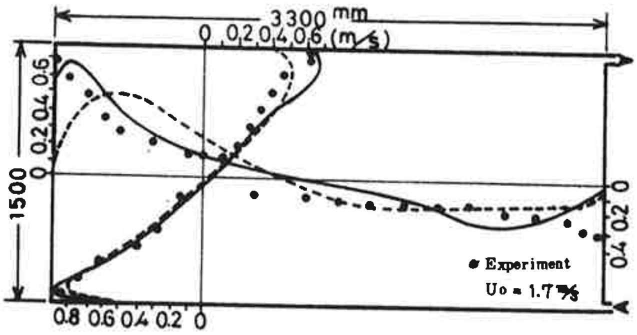

	r	C_2	ℓ-Type
(i) ———	1.0	1.0	II
(ii) - - - -	4.0	1.0	I

(c) Velocity Distributions

Fig. 9 Comparison of Flow Pattern and Velocity Distributions between Computed and Experiment in Case 1

Fig. 10 Comparison of Flow Pattern and Velocity Distributions between Computed and Experiment in Case 2

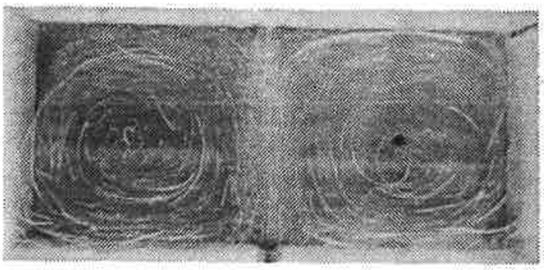

(a) Flow Pattern, t = ½ sec, f = 2.8

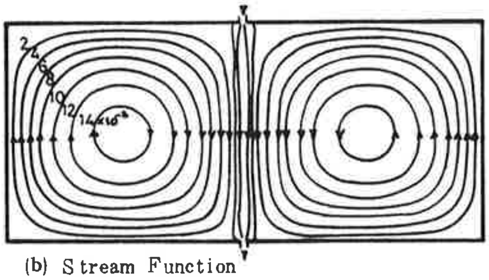

(b) Stream Function

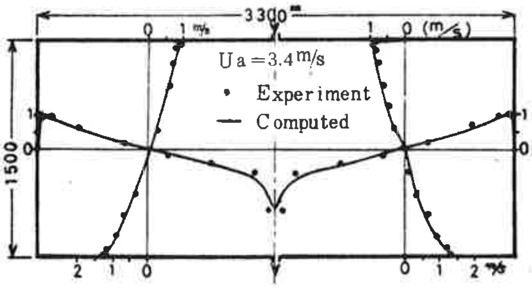

(c) Velocity Distribution

Fig. 11 Comparison of Flow Pattern and Velocity Distribution between Computed and Experiment in Case 3

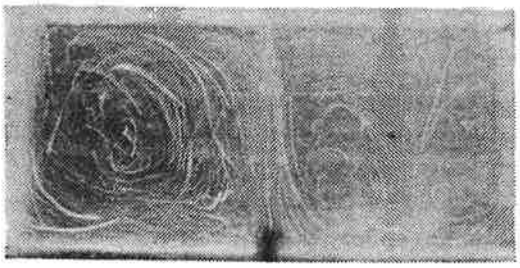

(a) Flow Pattern, t = ½ sec, f = 2.8

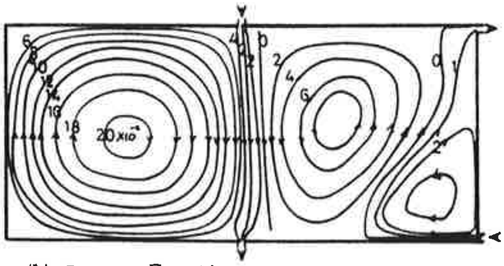

(b) Stream Function

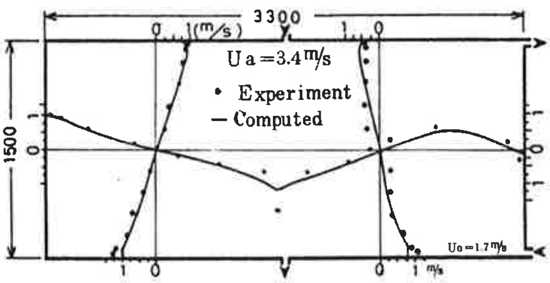

(c) Velocity Distribntion

Fig. 12 Comparison of Flow Pattern and Velocity Distribution between Computed and Experiment in Case 4

It can be concluded from the sections 5-1 - 5-3 that the best fitted values of γ and C_2 are 1.0 and 0.1, respectively, for the numerical calculation of two-dimensional room air motion with box model type finite differencing scheme, providing that the coefficient C_1 can be estimated by the knowledge of smooth plate flow. In the later section, the comparison will be made between the experiments and the calculations using the values $\gamma = 1$, $C_2 = 0.1$.

5-4 Flow Pattern

The calculated stream patterns for Case 1 and 2 are illustrated in Fig. 9 (b) and Fig. 10 (b). They are corresponding to the solid line in Fig. 9 (c) and Fig. 10 (c). The agreement between the calculated and the photoes taken by flow visualization technique is remarkable.

5-5 Application to Other Cases

The numerical calculations were applied to other two cases. One is the case for the room air motion with the jet injected downward at the center of the ceiling which is called as an air curtain. The other is for the air motion where the air curtain is affected by the creeping flow along the floor. In both cases, the selected values of $\gamma = 1$ and $C_2 = 0.1$ were used. Comparisons between the calculations and experiments were indicated in Fig. 11 and 12. In both cases, the calculated velocities agree quite well with the experiments except the jet region. Furthermore, it can be observed that the flow patterns, also agree well.

6 Conclusions

The computer programming of the numerical calculations for two-dimensional room air movements was developed by means of a box model finite differencing scheme for advection terms and the leapfrog time marching scheme.

Where three parameters were proposed. One was related to the eddy kinematic viscosity and the others were to correct the velocity and the vorticity gradients on a wall represented by a finite scheme. Two types of mixing length distribution were also examined in connection with isotropic or non-isotropic turbulence model. Several kinds of these parameters were attempted in order to find the best fit values as compared with experiments.

The following conclusions are presented:

(1) The most appropriate value of γ is 1.0, which is an emperical constant when an eddy kinematic viscosity is expressed in the product of the cube of mixing length and the absolute value of vorticity gradient, $K_x = \gamma \ell^3 \left| \frac{\partial \Omega}{\partial x} \right|$. When γ

was smaller than 1.0, the computed quantities indicated an irregular osillation. That was believed to resolve a part of turbulence. On the contrary, for $r > 1$, a relatively large damping took place and the unrealistic feature of flow pattern was displayed.

(2) The Type II together with non- isotropic is recommended as a distribution of mixing length. That is derived on the assumption that a room air can be divided into two regions by the surface composed of a maximum velocity point, the wall boundary region and the free turbulent region.

(3) The suitable value is believed to be 0.1 or less as C_2 which corrects the discrepancy between an actual vorticity gradient on a wall and that represented by finite difference approximation, providing that C_1 , which corrects a velocity gradient on a wall, can be estimated by the manner similar to the smooth plate flow.

(4) The validity of these parameters was confirmed by comparing the calculated velocity profiles with experiments in applications of the numerical procedure discribed in this report to the room air movement with symmetrical air curtain and that affected by a side blow.

ACKNOWLEDGEMENTS

The author would like to acknowledge the assistance of Mr. H. Seto of the Environmental Engineering Section, Building Physics and Fire Division. His help in carring out the experiments was greatly appreciated. Also, wishes are extended to all students of Kogakuin University who helped in both calculations and experiments.

REFERENCES

1) A. Arakawa: "Computational Design for Long-term Numerical Integration of the Equations of Fluid Motion: Two-Dimensional Incompressible Flow", Part 1. J. Comp. Phys., 1966

2) J. O. Wilkes and S. W. Churchill: "The Finite-Difference Computation of Natural Convection in a Rectangular Enclosure", Am. Inst. chem. Eng. J. 12, 1966

3) K. E. Torrance and J. A. Rockett: "Numerical Study of Natural Convection in an Enclosure with Localized Heating from below-Creeping Flow to the onset of Laminar Instability", J. Fluid Mech., 36, 33, 1969

4) J. E. Fromm: "A Numerical Method for Computing the Non-Linear, Time Dependent, Buoyant Circulation of Air in Rooms", IBM Research RJ 732, 1970

5) Y. Ogura and A. Yagihashi: "A Numerical Study of Convection Rolls in a Flow between Horizontal Parallel Plates", J. Meteor. Soc. Japan, 47, 1969

6) S. V. Patankar and D. B. Spalding: "A Calculation Procedure for Heat, Mass and Momentum Transfer in Three-Dimensional Parabolic Flows", Int. J. Heat Mass Transfer, Vol. 15, 1972

7) K. Aziz and J. D. Hellums: "Numerical Solution of the Three-Dimensional Equations of Motion for Laminar Natural Convection", The Physics of Fluids, Vol. 10, No. 2, 1967

8) P. V. Nielson: "Berechnung der Luftbewegung in einem Zwangsbelufteten Raum", Gesundheits-Ingenieur, Vol. 94, 1973

9) T. Terai: "On Thermal Convection in a Room", Trans. Arch. Inst. Japan, No. 59, 1958

10) T. Tsuchiya and T. Shoda: "On the Method of Numerical Calculation of Room Air Motion", Proc. Annual Meeting Arch. Inst. Japan, 3088, 1968

11) H. Yamazaki, M. Nishida and Y. Urano: "Numerical Calculation of Room Air Flow - On the Method of Convergence", Proc. Annual Meeting Arch. Inst. Japan, 4202, 1972

12) T. Tsuchiya: "Approximate Solution of Room Thermal Convection", Ibid, 4206

13) M. Enai and N. Aratani: "Fundamental Consideration for Analysis of Room Thermal Convection", Ibid. 4204

14) M. Kaizuka, Y. Sakamoto et. al.: "Three-Dimensional Numerical Calculation of Turbulent Room Air Flow by means of Two-Equation Model", Proc. Annual Meeting Arch. Inst. Japan, 4154 - 4156, 1975

15) B. E. Launder and D. B. Spalding: "Mathematical Models of Turbulence", Academic Press, 1972

16) F. H. Harlow and P. I. Nakayama: "Turbulence Transport Equations", The Physics of Fluids, Vol. 10, 1967

17) Y. Kurihara and J. L. Holloway: "Numerical Integration of a Nine-Level Global Primitive Equations Model Formulated by the Box Method", Mon. Weath. Rev., 95, 1967

18) K. Bryan: "A Scheme for Numerical Integration of the Equations of Motions on an Irregular Grid free of Non-Linear Instability", Mon. Weath. Rev., 94, 1966

19) D. K. Lilly: "On the Computational Stability of Numerical Solutions of Time Dependent Non-Linear Geophysical Fluid Dynamics Problems", Mon. Weath. Rev., 93, 1965

20) R. D. Richtmyer and K. W. Morton: "Difference Methods for Initial-Value Problems", Interscience Publishers, 1967

21) L. F. Daws: "Movement of Air Streams Indoors", J.I.H.V.E., Vol. 37, Feb. 1970

Research Papers–recent issues

No. 45 K. Kawagoe: Charts for Estimating the Equivalent Fire Duration on the Standard Temperature-Time Curve, January 1971, 190pp.
No. 46 T. Wakamatsu: Calculation of Smoke Movement in Buildings – Second Report, March 1971, 23pp.
No. 47 M. Ozaki: Axisymmetric Plane and Plate Stress Analysis by Framework Method, March 1971, 41pp.
No. 48 Research Planning Group: General Aspects of Building Research in Japan, March 1971, 87 pp.
No. 49 [illegible] Koizumi, M. Hirosawa, S. Okamoto, Y. Matsushima, T. Endo: Lateral Load Tests on Multi-Storied Full-Size Building of Reinforced Concrete Wall Construction for Earthquake Resistant Design, March 1971, 12 pp.
No. 50 M. Ozaki, H. Iwasaki: Proposal for Offshore Building Standards, August 1971, 26pp.
No. 51 Y. Ohsaki, M. Watabe, [illegible]: On Structural Inelastic Response and Human Response in Relation to the Maximum Acceleration of [illegible] the Earthquakes, October 1971, 23pp.
No. 52 F. Seo, S. Yoda: The Performance of Open Joints, March 1972, 31pp.
No. 53 H. Saito: Fire Resistance Design for Steel Structures, May 1972, 36pp.
No. 54 T. Wakamatsu: Design of Fire Cover on Steel Structures, May 1972, 14 pp.
No. 55 Research Group for Systematic Method for Selecting Building Materials: A Systematic Method for Selecting Building Materials – Performance Testing Methods for Building, Building Elements, Components and Materials –, March 1973, 138 pp.
No. 56 K. Nakano, M. Hirosawa: BRI Standard for Earthquake Resistant Properties of Existing Reinforced Concrete Buildings, 1974, 23 pp.
No. 57 M. Hirosawa, T. Endo: Experimental Research on Ductility of Reinforced concrete Columns, February 1974, 38 pp.
No. 58 Y. Matsushima: Stochastic Response of Structure Due to Three-dimensional Earthquake Excitations, March 1974, 16pp.
No. 59 Y. Aoki: Mathematical Formulations and Analyses on Client's Wills and Planning processes, March 1974, 33 pp.
No. 60 Y. Aoki: Scenario-Writing Method As a Systematic Evaluation Method for Building Production, July 1974, 48pp.
No. 61 T. Wakamatsu: Smoke Movement in Building Fires – Field Experiment in Welfare Ministry Building and Analysis of Seamen's Building Fire –, February 1976, 24 pp.
No. 62 T. [illegible]: Numerical Calculation on Room Air Movement, January 1976, 28 pp.
No. 63 K. Inazumi: Summary of Research and Development for Wood Frame Construction in 1975, January 1976, 18 pp.
No. 64 M. Ozaki, [illegible]: An Evaluation Method for the Earthquake Resistant Capacity of Reinforced Concrete and Steel Reinforced Concrete Columns, February 1976, 38pp.

Printed [illegible]

Address for Communication

BUILDING RESEARCH INSTITUTE

MINISTRY OF CONSTRUCTION, JAPANESE GOVERNMENT

[illegible]

TOKYO, JAPAN